Voids growth and coalescence fracture mechanism computational study by discrete element method

Ruben Galiano Batista[1], Ignacio Iturrioz[1] and Adrián P. Cisilino[2]

[1] PROMEC, Universidade Federal do Rio Grande do Sul
Sarmento Leite 425, Porto Alegre, Brazil

[2] División Soldadura y Fractomecánica – INTEMA
Facultad de Ingeniería, Universidad Nacional de Mar del Plata
Av. Juan B. Justo 4302 - (B7608FDQ) Mar del Plata, Argentina

Abstract

The micromechanics of fracture by growing and coalescence of voids is described using the discrete element method (DEM) for micro-porous metal-matrix material. The study was developed in a series of representative volume elements (RVE) of a pseudo-microstructure of the reference material. In the RVEs, the stress vs strain, damage energy, elastic strain energy response and the evolution of the void volume fraction were analysed. Differently from other criteria encountered in literature, in this work, the occurrence of coalescence is considered, when two voids merge completely. Special attention is given to the moment of coalescence and final failure. The values of the void volume fraction at the coalescence are in good agreement with other visited reports. The results obtained demonstrate de effectiveness of the DEM in the modelling of fracture modes involving growth and void coalescence.

Keywords: micro-porous metal-matrix material, discrete element method, damage mechanics

1 Introduction

The fracture micromechanics process of the metallic material has been divided into the following stages: nucleation, growth and coalescence of voids that are originated from the non metallic inclusion or second phase particles present in the metallic microstructure.

In materials where there is a hard interaction between the particle and metallic matrix, the nucleation stage is a determinant one in the fracture process. When the interaction particle – metallic matrix is weak, the determinant stage in the fracture process is the voids coalescence (Anderson, 1991). It is on this kind of material that the present work focuses.

Direct experimental observation of any fracture micromechanics evolution is very difficult, due to the scale in which this process occurs, which led to a few citation references about in situ observation of this evolution process (Berdin et al., 2001).

The computational mechanics has **shown** itself as an efficient tool to help the physical experimentation related to the interaction among voids phenomena. In this context, many works have been carried out. As examples, it is possible to indicate the proposal that the material void volume fraction *(f)* is considered as a parameter of the constitutive models, (Gurson 1977), and the verification of the influences of the mechanical-metallurgical parameters such as: the initial void volume fraction f_0, shape and size voids, the influence of the stress triaxiality level, etc, in the growing and coalescence voids, (Kim et al, 2004).

Considering that most works carried out in this area use the Finite Element Method and that in those studies the material periodicity is taken into account, the main aim of the present work is to verify the DEM applicability to the simulation of the voids growth and coalescence fracture mechanism for random microstructures materials.

To accomplish this aim, 2D-model representative volume elements (RVE) of a Ferritic Nodular Cast Iron pseudo-microstructure were built and, in these models, the mechanics response evolution was simulated and the result in terms of void volume fraction *f* evolution was obtained. Henceforward, the criteria to voids coalescence and to rupture are proposed.

The basic characteristics about the DEM could be found in (Iturrioz et al 2006), a work presented in the same Conference.

2 Topological characterization of the reference material microstructure.

The reference material used to build DEM models was the Ferritic Nodular Cast Iron (FNCI). The graphite nodules distribution characterization was carried out from the statistical analysis of the FNCI micrographies (Fig. 1a), considering the nodules with perfect circular shape as an accepted simplification and different number of nodules per unit area (from 60 tol 600 nodules/mm2). The analyzed nodules distributions parameters was, the nodules radii (*r*), nearest neighbors distance (d), nearest neighbors number (N), and mean nearest neighbors distance (see Fig. 1(b)).

The number of the nearest nodule neighbors and the nodule center position were determined using a Delaunay Algorithm. The process is illustrated in Fig.1(b,c,d).

Taking into account a previous statistical study, it may be concluded that the distribution of nodules is almost independent on the nodular count when the ratio *d/r* is chosen as a parameter. Based on this conclusion, and bearing in mind that the 3D volume fraction of spherical inclusions of a representative volume element coincides with the 2D volume fraction (area fraction) of its cross section (Sevostionov et al., 2004), the nodule radius *r* was chosen as the characteristic length for the generation of the geometries of the DEM models. Thus, the model geometries consisted in random distributions of non-overlapping nodules of identical size, Fig.1 (d). This geometry

possesses mean values for $(d/r)_{cl}$ = 3.91, $(d/r)_{nat}$ =6.99 and N= 5.96, which are well in accordance with those computed from the micrographs. This correspondence was verified for the computer generated models in all the range of node counts N_{area}.

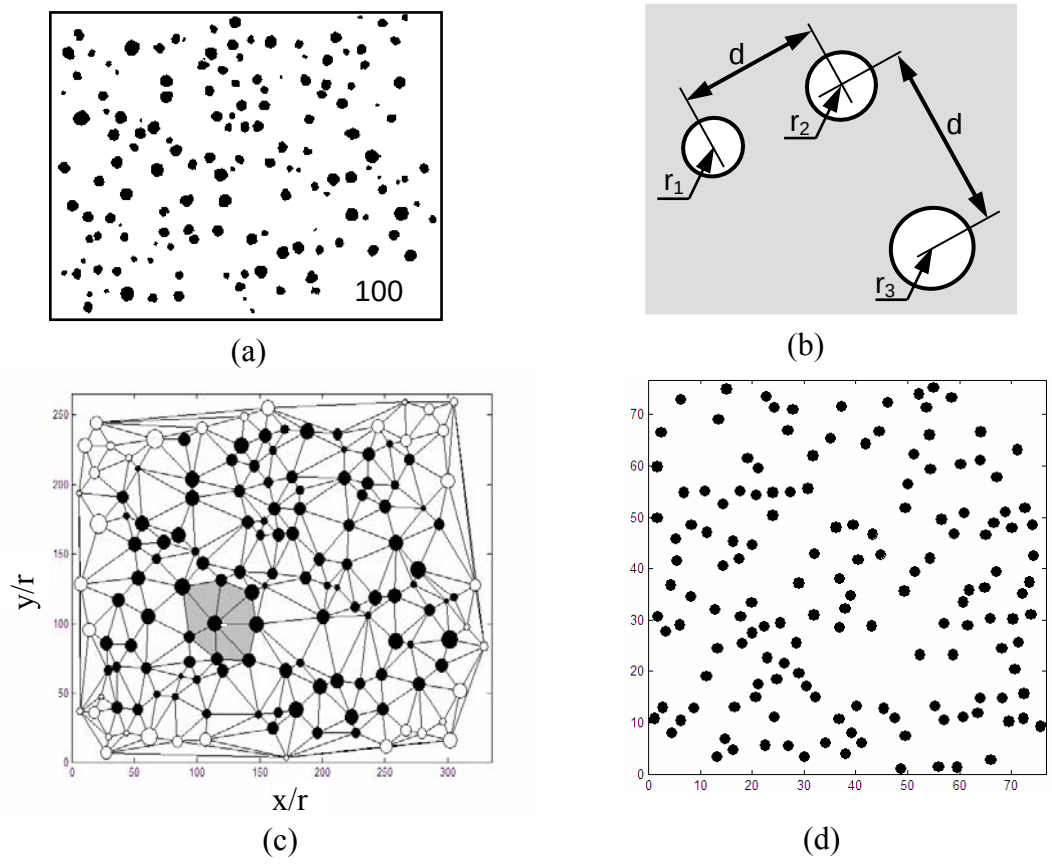

Figure 1: (a) Micrograph without etching of nodular cast iron. (b) Geometrical parameters used in the geometrical characterization of the microstructure, (c) Delaunay triangulation of the positions of the nodules for the micrograph shown in (a), and (d). Example of a randomly generated microstructure containing 150 nodules.

In table 1, the FNCI material properties utilized in the DEM models are depicted.

Tabela 1. Mechanical properties of reference material (Berdin 2001)

E (MPa)	σ_u (MPa)	σ_y (MPa)	Elongation %	K_{IC} (MPa·m$^{1/2}$)	f_0 %
187000	390	260	23	77	7,7

3.2 Void volume fraction computation

Since the graphite has a very low mechanical strength if compared to the matrix strength, and in the FNCI, taken as a reference material, the unsticking nodule-matrix happens at the beginning of the plastic strain (Berdin 2001). The simulated model can be considered as a microporous material. Then, in DEM models, load transmition capacity of those bars corresponding to nodules regions was diminished (see Fig 2).

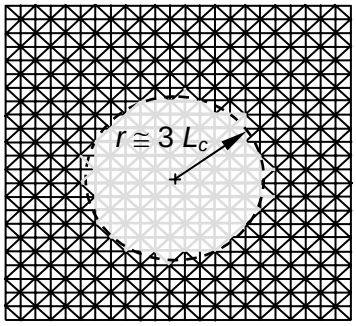

Figure 2: Procedure for the introduction of initial voids into the DEM model (Note that only those elements with their centroids located within the nodule domain are selected and weakened).

Using three DEM cubic modules per radii, it was possible to obtain a good geometric representation of the nodules. The initial voids volume and its growth during the damage evolution in the simulated process was defined by Eq. 1. In Eq. 1, *Vi* represents a cubic module volume, $n^i_{weakened}$ represents the number of the weakened bars that correspond to the analyzed module, n^i_{failed} represents the number of the failed bars that correspond to the analysed module, and, finally, the n^i_{total} corresponds to the total number of bars of one module. If the module is not a boundary module, then $n^i_{total} = 26$.

$$f = \frac{\sum_{i=1}^{m} V_i \cdot \frac{n^i_{weakened}}{n^i_{total}} + \sum_{i=1}^{m} V_i \cdot \frac{n^i_{failed}}{n^i_{total}}}{\sum_{i=1}^{m} V_i} \qquad (1)$$

4. Determination of the representative volume element

The Representative Volume Element (RVE) is the smallest material volume that presents a macroscopic invariant response. The material sample must be big enough to contain a high number of heterogeneities (graphite nodules in this case) and to present little response ranges caused by boundary irregularities (Terada and Kikuchi, 1995).

To obtain the RVE, a set of DEM simulations of the Pseudo FNCI Microstructures were carried out, containing the increasing number of nodules but keeping the void fraction volume constant. Ten configurations with different nodules distribution were tested by each sample size. The biaxial tensile boundary condition was applied on these samples; hence the Hill (1952) condition was fulfilled.

The field parameters verified in the RVE determination were a strain elastic energy density, $u_{el} = U_{el}/V$, the Damage energy density $u_{damage}=U_{damage}/V$, and the void volume fraction *f*. These control parameters were computed in different stages of the loading process, as indicated by the following characteristic points: P1- in the linear elastic regime-, P2- non linear regime-, and P3- in the maximum stress, (Fig. 6 (a)).

The obtained results in the RVE determination are shown in Fig 3 and 4, in terms of the mean values corresponding to ten analyzed simulations for each sample size considered. The dispersion of each value is represented by the error bar in the same plots.

The control points P1, P2 and P3 show a stable behavior in terms of strain elastic density energy (u_{el}) from the 30 nodules samples, with an approximated dispersion of about 0,5 %, 8 % e 30 %, respectively, as shown in Figs. 3 (b), 3 (c) e 3 (d)).

The behavior evidenced for the density damaged energy u_{damage} in the control points P1, P2 and P3 ((Figs. 4(a) e 4(b)), shows convergence and dispersion characteristics similar to the results in terms of strain elastic density energy (u_{el}), at the same stages of

loading.

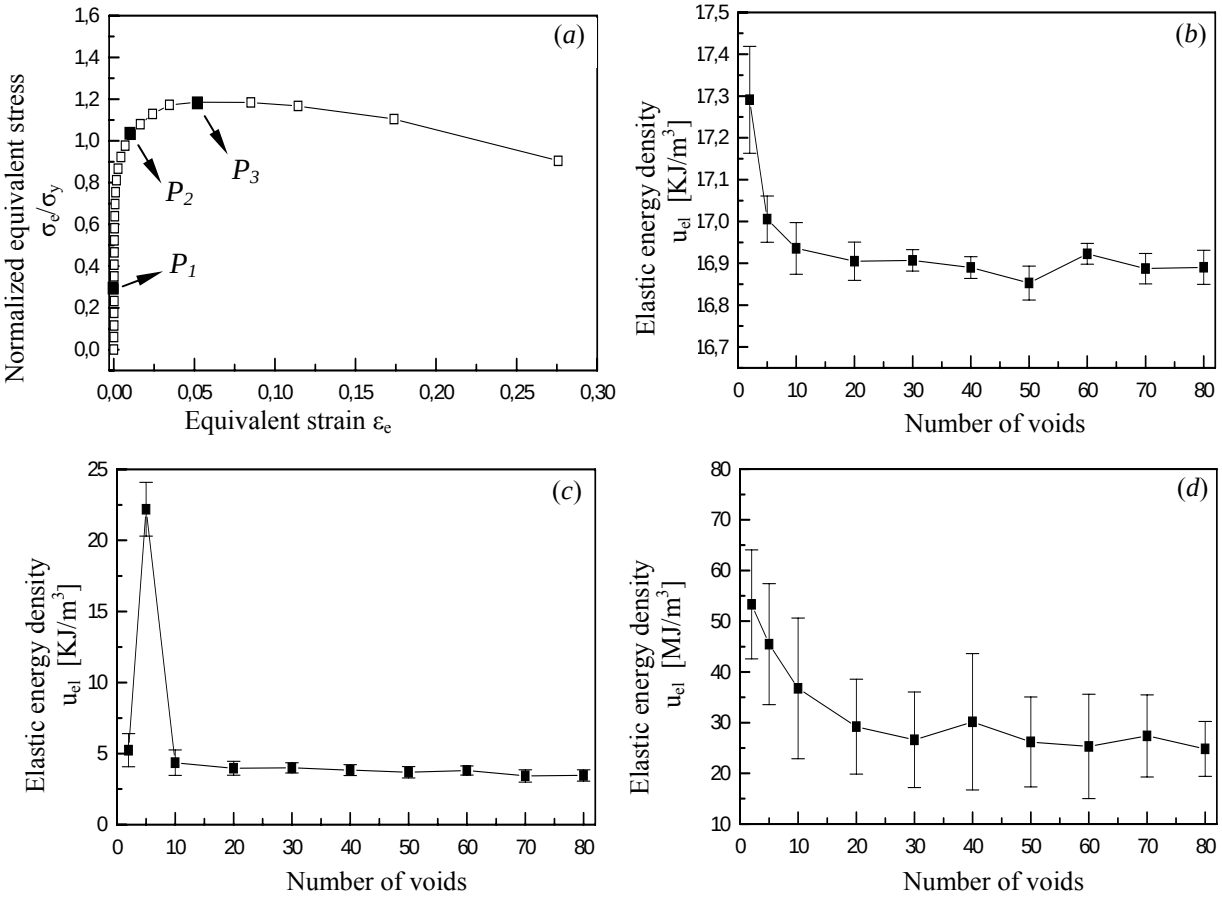

Figure 3: The RVE scheme determination. (a)The location of the control points in the stress-strain curve. The results in terms of the strain elastic energy density u_{el}.: (b) the linear regime (P1), (c) The non linear regime (P2), and (d) the maximum stress (P3).

In the case of the void volume (Fig. 4(c)), for control points P1 and P2, it is possible to observe convergence in terms of the mean response from 20 nodules sample, with an approximated dispersion of 0,2% for both control points. On the other hand, in control point P3, the convergence from 40 nodules samples with an approximated dispersion of 30% is observed.

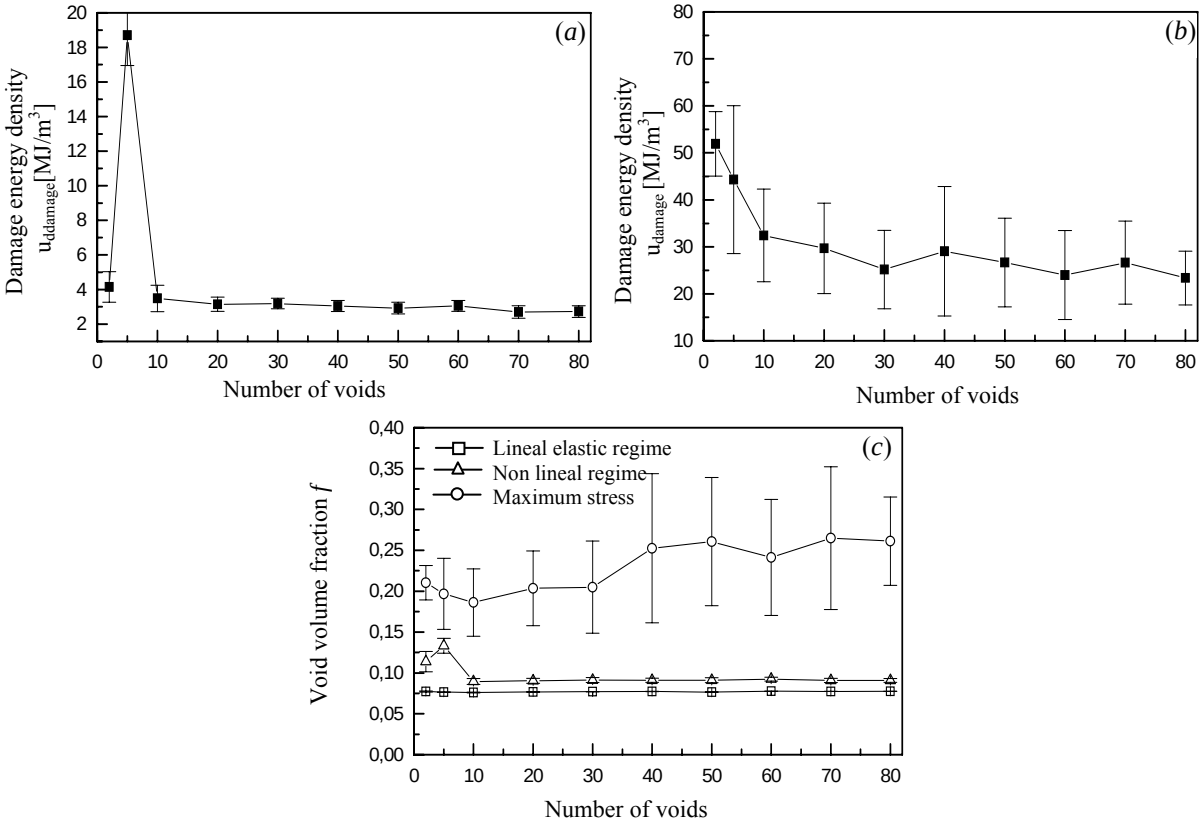

Figure 4: Results in terms of damage energy density u_{damage} and fraction void volume f for the samples with different number of nodules. (a) u_{damage} in the non linear control point (P2),(b)) u_{damage} in the maximum stress control point (P3). (c) f in the three control point (P1,P2,P3). The error bar indicates the dispersion in the result obtained.

Henceforward, it is possible to consider that a sample with 40 nodules presents a mechanical response with an acceptable level of scattering. The using of the bigger samples increases the computational cost without significant improvement not only in terms of dispersion result, but also in terms of the mean values of the field variables considered. According to the above facts, it is possible to conclude that a 40 nodules sample might be considered as an RVE of the pseudo micro structure of the FNCI.

5. Application to tension test

Forty RVEs DEM models containing 40 nodules each were subjected to uniaxial traction in order to study the evolution of the damage in the pseudo-micro-structure.

Fig. 5 illustrates the mean value and standard deviation (y-error bars) of the resulting stress vs strain curve together with the actual behaviour of one sample reference material.(Berdin et al, 2001). It can be observed that the numerical and experimental results are in excellent agreement up to the point where the maximum load is attained in the numerical models ($\varepsilon_{22} \approx 0{,}12$) and then start diverging. However, experimental data are always contained within the standard deviation of the numerical results.

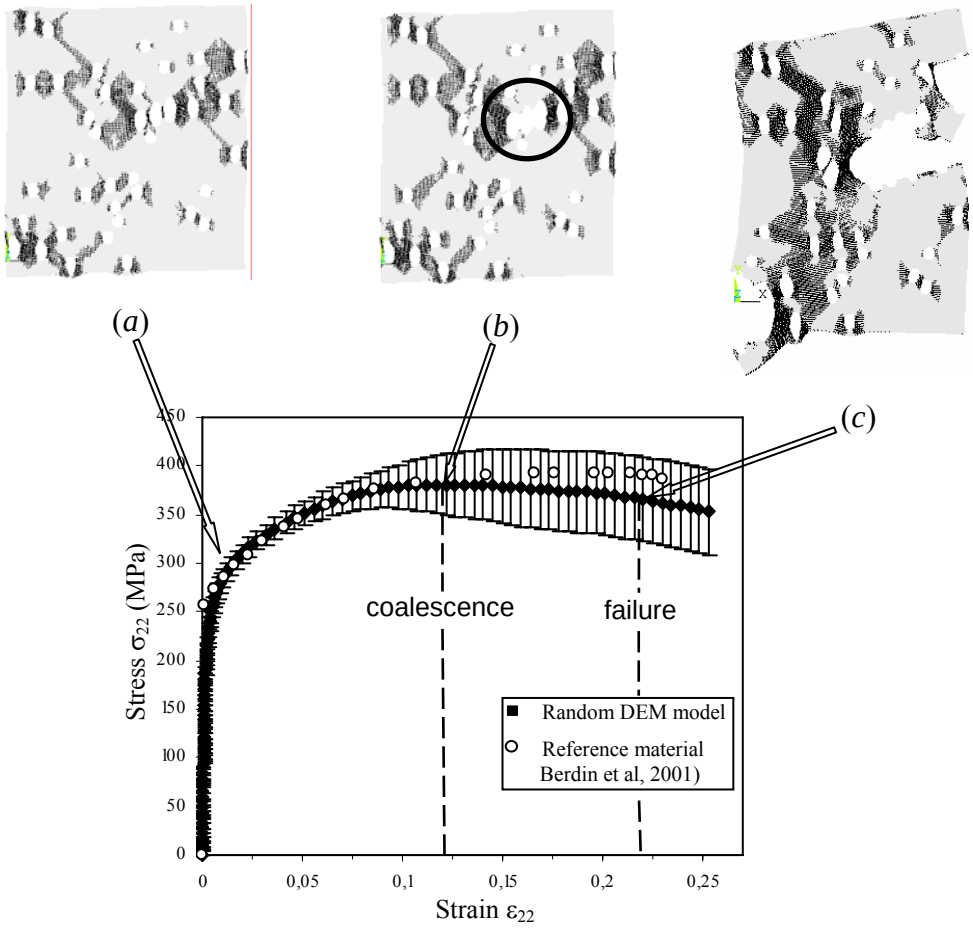

Figure 5: Mean value and standard deviation (y-error bars) of the uniaxial stress vs strain curve resulting from DEM analyses for the forty random RVE and the regular microstructure. Subfigures illustrate the evolution of the damage with the applied load.

The evolution of the damage in the microstructure for the random models is depicted using a series of subfigures in Fig. 5. Black areas in the subfigures correspond to the

damaged elements. Subfigure (*a*) shows the location of the damage in the early stages of the non-linear portion of the stress vs strain curve. Beginning the coalescence shows in subfigure (b) (circled detail) and ends in subfigure (*c*), illustrating the stage of advanced damage.

5.1 Coalescence verification.

Coalescence is considered to occur in this work when the complete failure of the ligament between the voids takes place. This criterion aims to quantify the actual void fraction in the model at the onset of coalescence (f_c), and it differs from others criteria reported in the literature, with values from $f_c = 0.10$ to $f_c = 0.20$ (Tvergaard and Needleman, 1984; Goods and Brown, 1979; Kim et al, 2004).

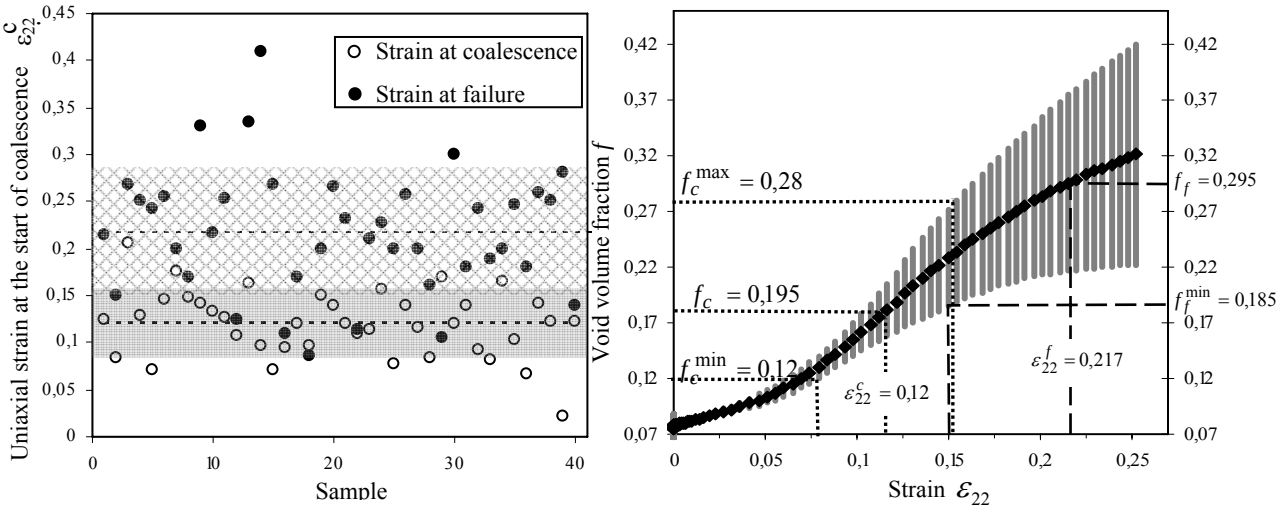

(a) (b)

Figure 6: Onset of coalescence and failure a) Strain at moment of coalescence and failure for the forty EVRs (The dashed line and the shaded band indicate mean value and standard deviation of the results, respectively and b) Evolution of the void volume fraction as a function of the longitudinal strain

The strain at the occurrence of coalescence for all the forty RVE models is shown in Figure 6 (a). The average macroscopic strain value for the onset of coalescence is $\varepsilon_{22}^{c} = 0.12$ with a standard deviation Δ=±0.035 (see shaded band in Figure 6).

Note that the average strain value for coalescence, ε_{22}^{c}, corresponds to the maximum load attained by the numerical models (Fig. 5).

Fig.6 (b) illustrates mean evolution of the void volume fraction in terms of the longitudinal strain ε_{22}, with y-error bars indicating the results dispersion. The strain range corresponding to the onset of coalescence (Fig.6), was used to estimate the critical void volume fraction f_c. The resulting mean value for the critical void volume fraction is $f_c = 0.19$, with lower and upper bounds $f_c^{\min} = 0.12$ and $f_c^{\max} = 0.27$, respectively. As mentioned early in this section, reported values for the critical void volume fraction are in the range from $f_c = 0.10$ to $f_c = 0.20$. This upper bound is strongly influenced by the dispersion in the void volume fraction results, which as shown in Section 4, could be important once maximum load is attained

The void volume fraction at the onset of coalescence reported for the reference material is $f_c = 0.12$ (Berdin et al, 2001). This value results lower than the mean $f_c = 0.19$ computed in this work and a number of reasons could help explaining this discrepancy. The first consideration is related to the concept of coalescence itself. As stated earlier in this section, coalescence is considered to occur in the DEM models when two voids (nodules) merge, while the usual criteria in the literature associates coalescence of flow localization in the ligament between voids. Thus, it could be expected that the DEM models will detect coalescence "later" during the loading process**.** At the same time it is worth to note that the value of f_c reported by Berdin et al, (2001) does not correspond to actual experimental observations, but it was calibrated in order to adjust a Gurson model

to the test data. Another important issue to consider when comparing the DEM results to that of Berdin et al, (2001) is stress triaxiality. It is well known that Gurson model assumes a high level of stress triaxiality and the dependence of f_c on stress triaxiality is pronounced. Kim et al, (2004) report increments of up to 80% in f_c when reducing the stress triaxility for a material containing an initial volume fraction f_o= 0.05. They also show that this tendency can further increase when augmenting the initial volume fraction. Thus, if it is considered that computations in this work are performed for RVEs subjected to low triaxiality levels (two-dimensional plane-stress models) with an initial void volume fraction f_o= 0.077, relatively high levels of the critical void volume fraction could be expected.

5.1 Failure verification.

The final failure was monitored for the forty RVE and the results in terms of the macroscopic strain are presented in Fig. 6 (a). The mean value for the failure strain is $\varepsilon_{22}^{f} = 0.217$ with a standard deviation of Δ=± 0.067, in close agreement with the elongation values reported by Berdin et al (2001) (see Table 1).

The strain range for failure was used to estimate the void volume fraction at failure f_f (see Fig. 6 (b)). The resulting mean value is $f_f = 0{,}295$, with lower and upper bounds $f_f^{\min} = 0{,}185$ and $f_f^{\max} = 0{,}42$, respectively. When compared to the results reported by Berdin et al (2001) and Dong et al (1997), for the reference material, f_f = 0.20, is almost coincident with the computed lower bound. The relatively large dispersion encountered for the results at failure can be partially attributed to the size of the RVE.

5.2 Three-dimensional verification.

Because it was taken as premise that the RVE obtained in the 2D analysis is valid in 3D, a 3D-analysis with five samples of 40 nodules of a pseudo microestructure of FNCI was carried out. Fig 7 illustrates the lay out of the 3D-DEM samples.

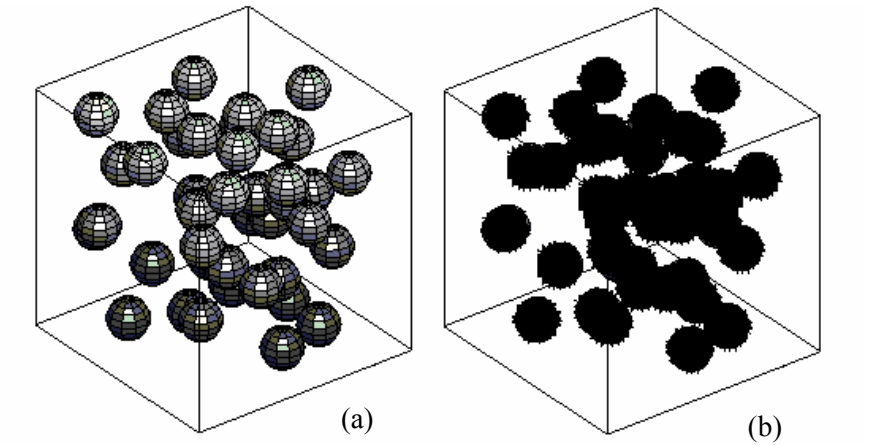

Figure 7: The nodules distribution in 3D. a) The automatic distribution generated, b) The correspondent DEM model Sample.

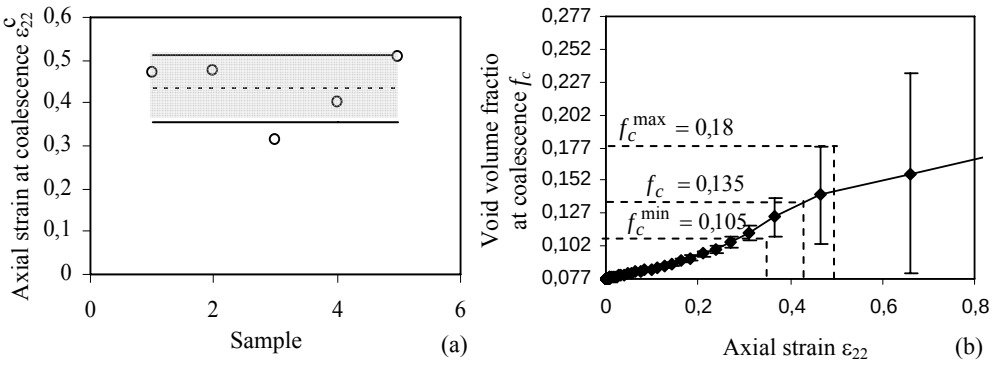

Figure 8. Onset of coalescence in 3D. a) Axial strain at coalescence b) Void volume fraction at coalescence.

In the same way as for the 2D analysis, in the 3D analysis, were verified a strain when the coalescence happens, as illustrated in Fig. 8(a). By means of this characteristic strain value, it is possible to obtain the correspondent void volume fraction f_c, as shown in Fig. 8(b). It is possible to observe that the *fc* verified in the 3D models is lower than the *fc*

obtained in the 2D models. This statement is coherent with the theoretical response obtained considering a comparison between a circular planar void arrangement and a sphere void arrangement, both with regular distribution. Similar tendency in the result of the 3D and 2D were found by other authors such as Kim et al. (2004).

6. Conclusions

A Discrete Element Method (DEM) formulation for the analysis of the micro-mechanics of failure by grow and coalescence of voids was presented in this paper. The DEM was selected for the numerical analyses due its inherent ability to handle crack nucleation and void coalescence. The microstructure of the cast iron was assimilated to that of porous materials, with the graphite nodules acting as voids in an elastic-plastic matrix. The topology of the microstructure was characterized from the statistical analysis of measurements performed on standard micrographs using image-processing. DEM models were carried out using two-dimensional computer-generated microstructures which reproduce the distribution of nodules of the material.

The size of the Representative Volume Element (RVE) was determined using a series of DEM models performed for samples containing an increasing number of nodules. The strain energy density, the damage energy density, and the void volume fraction were monitored throughout the tests till an invariant macroscopic response was found for the linear and non-linear regimes. Finally, a RVE containing 40 nodules was selected.

The extension for a 3D analysis is possible; the great limitation, in this case, is the computational cost.

The proposed methodology demonstrates the effectiveness of the DEM to provide further understanding of the micro-mechanics of failure by grow and coalescence of voids. The developed tool could be easily adapted to include the effect of inclusions,

inhomogeneities in the matrix mechanical properties, viscous effects and to extend this tool to three dimensional problems.

Acknowledgements

This work was partially supported by grants CAPES/SECYT BR/PA02-EXII/007 (Fundaçao Coordenaçao de Aperfeiçoamento de Pessoal Nivel Superior, Brazil and Secretaría de Ciencia Técnología e Innovación Productiva, Argentina), PROSUL 040/2006 (Conselho Nacional de Desenvolvimento Científico e Tecnológico, Brazil) and PICT 12-12528 (Agencia de Promoción Científica y Tecnológica de la República Argentina).

Referentes

- Berdin C., Dong M.J. and Prioul C., Local approach of damage and fracture toughness for nodular cast iron, *Engineering Fracture Mechanics*, 68, 1107-1117 (2001)

- Dong M. J, Prioul C. and François D. Damage Effect on the Fracture Toughness of Nodular Cast Iron: Part I. Damage Characterization and Plastic Flow Stress Modelling, *Metalurgical and Materials Transaction A*, V. 28ª, 2245 – 2254 (1997)

- Goods S. H. and Brown L. M., The nucleation of cavities by plastic deformation, *Acta Metallurgica* Vol 27, Issue 1, 1-159 (1979)

- Gurson, A. L., Continuum Theory of Ductile Rupture by Void Nucleation and Growth: Part I- Yield Criteria and Flow Rules for Porous Ductile Media, *Journal of Engineering Materials and Technology*, Vol. 99, 2-15 (1997)

- Hill, R., The Elastic Behavior of a Crystalline Aggregate. *Proc. Phys. Soc.* A65, 349-354, London (1952).

-Iturrioz I., Morquio A., Bittencourt E. and Rosito d'Avila V., M., Performance of the discrete element method to represent the scale effect. Mecsol 2007.

- Kim K., Gao X. and Srivtsan T., Modeling of void growth in ductile solids: effects of stress triaxiality and initial porosity, *Engineering Fracture Mechanics*, 71, 379-400 (2004).

- Kouznetsova V., Brekelmans W.A.M., and Baaijens F.P.T., An approach to micro-macromodelling of heterogeneous materials. Comput. Mechanics, 27, 37-48 (2001)

- Sevostionov I., Agnihotri G. and Flores Garay J., On connections between 3-D Microstructures and their 2-D images, *International Journal of Fracture*, 126: 65-72 (2004).

- Anderson T. L., Fracture Mechanics: Fundamentals and Applications, Departament of Mechanical Engineering, Texas A&M University, College Station, Texas, 1991

- Terada K. Kikuchi N., Nonlinear homogenization method for practical applications In: *Computational Methods in Micromechanics* (eds. Ghosh S., Ostoja-Starzewski M.), AMD-Vol. 212/MD-Vol. 62, ASME, 1-16 (1995)

- Tvergaard V. and Needleman A., Analysis of the cup-cone fracture in a round tensile bar. *Acta Metallurgica*, Vol 32, 157-169 (1984)